

Iron suppresses erythropoietin expression via oxidative stress-dependent hypoxia-inducible factor-2 alpha inactivation

Keisuke Oshima^{1,2,9}, Yasumasa Ikeda^{1,9}, Yuya Horinouchi¹, Hiroaki Watanabe³, Hirofumi Hamano^{1,4}, Yoshitaka Kihira^{1,5}, Seiji Kishi⁶, Yuki Izawa-Ishizawa¹, Licht Miyamoto⁷, Tasuku Hirayama⁸, Hideko Nagasawa⁸, Keisuke Ishizawa^{3,4}, Koichiro Tsuchiya⁷ and Toshiaki Tamaki¹

Renal anemia is a major complication in chronic kidney disease (CKD). Iron supplementation, as well as erythropoiesis-stimulating agents, are widely used for treatment of renal anemia. However, excess iron causes oxidative stress via the Fenton reaction, and iron supplementation might damage remnant renal function including erythropoietin (EPO) production in CKD. *EPO* gene expression was suppressed in mice following direct iron treatment. Hypoxia-inducible factor-2 alpha (HIF-2 α), a positive regulator of the *EPO* gene, was also diminished in the kidney of mice following iron treatment. Anemia-induced increase in renal *EPO* and HIF-2 α expression was inhibited by iron treatment. In *in vitro* experiments using EPO-producing HepG2 cells, iron stimulation reduced the expression of the *EPO* gene, as well as HIF-2 α . Moreover, iron treatment augmented oxidative stress, and iron-induced reduction of *EPO* and HIF-2 α expression was restored by tempol, an antioxidant compound. HIF-2 α interaction with the *Epo* promoter was inhibited by iron treatment, and was restored by tempol. These findings suggested that iron supplementation reduced *EPO* gene expression via an oxidative stress-HIF-2 α -dependent signaling pathway.

Laboratory Investigation (2017) **97**, 555–566; doi:10.1038/labinvest.2017.11; published online 6 March 2017

The incidence of chronic kidney disease (CKD) has increased worldwide, and CKD worsens morbidity and mortality in the general population.^{1,2} The progression of CKD results in end-stage renal failure, which requires treatment by hemodialysis or renal transplantation. In addition, a variety of complications arises during the course of CKD. Cardiovascular disease, a major complication of CKD, also leads to worse outcomes in CKD patients.³ Renal anemia is commonly seen in individuals with CKD due to insufficient erythropoietin (EPO) production within the diseased kidney.^{4,5} Therefore, patients with end-stage renal disease receive erythropoiesis-stimulating agent (ESA) for the treatment of renal anemia.

Iron supplementation, in addition to ESA, is often used for the treatment of renal anemia.⁶ However, patients with CKD

often show functional iron deficiency, rather than absolute iron deficiency, characterized by impaired iron release from body iron stores.⁷ Disturbance of iron utilization in CKD occurs due to ferroportin (a cellular iron exporter) degradation resulting from increased hepcidin production.^{8,9} Hepcidin is positively controlled by iron stores.¹⁰ Therefore, iron treatment further exacerbates impaired iron utilization via hepcidin elevation and results in over accumulation of disused iron in organs of CKD individuals. Actually, adverse effects of iron supplementation on organs have been directly observed in several studies. Iron sucrose treatment exacerbates endothelial dysfunction in healthy subjects¹¹ and atherosclerotic change through enhancement of oxidative stress in a CKD mouse model.¹² Intravenous iron also causes

¹Department of Pharmacology, Institute of Biomedical Sciences, Tokushima University Graduate School, Tokushima, Japan; ²Student Lab, Tokushima University Faculty of Medicine, Tokushima, Japan; ³Department of Clinical Pharmacy, Institute of Biomedical Sciences, Tokushima University Graduate School, Tokushima, Japan; ⁴Department of Pharmacy, Tokushima University Hospital, Tokushima, Japan; ⁵Department of Clinical Pharmacy, Faculty of Pharmacy and Pharmaceutical Sciences, Fukuyama University, Fukuyama, Japan; ⁶Department of Nephrology, Institute of Biomedical Sciences, Tokushima University Graduate School, Tokushima, Japan; ⁷Department of Medical Pharmacology, Institute of Biomedical Sciences, Tokushima University Graduate School, Tokushima, Japan and ⁸Laboratory of Pharmaceutical and Medicinal Chemistry, Gifu Pharmaceutical University, Gifu, Japan

Correspondence: Y Ikeda, MD, PhD, Department of Pharmacology, Institute of Biomedical Sciences, Tokushima University Graduate School, 3-18-15 Kuramoto-cho, Tokushima 770-8503, Japan.

E-mail: yasuike@tokushima-u.ac.jp

⁹These authors equally contributed to this work.

Received 19 August 2016; revised 16 January 2017; accepted 16 January 2017

oxidative stress and transient proteinuria, tubular damage, and inflammatory cytokine production in patients with CKD.^{13,14} Thus, parenteral iron supplementation might aggravate and cause complications in CKD through oxidative stress production. Furthermore, iron might exacerbate erythropoietin production consequent to remnant kidney injury, however, the effect of iron on EPO regulation has not been elucidated.

Here, we demonstrate that saccharated ferric oxide (SFO) reduced renal *EPO* expression through iron-induced oxidative stress production-dependent inactivation of hypoxia-inducible factor-2 α (HIF-2 α). Our findings suggest that therapeutic iron supplementation has a harmful effect on EPO regulation in remnant kidney function, causing a vicious cycle of CKD progression.

MATERIALS AND METHODS

Materials

We purchased saccharated ferric oxide (SFO), cobalt chloride (CoCl₂), tempol, and dimethylallyl glycine (DMOG) from Nichi-Iko Pharmaceutical, Co., Ltd. (Toyama, Japan), Wako Pure Chemical Industries (Osaka, Japan), Sigma-Aldrich (St Louis, MO, USA), and Cayman Chemical Company (Ann Arbor, MI, USA), respectively. The following commercially available antibodies were used: anti-HIF-2 α (R&D Systems, Minneapolis, MN, USA); anti-HIF-1 α (Cayman Chemical); anti-PDGF-R β (Cell Signaling Technology, Beverly, MA, USA); anti- α -SMA (Sigma-Aldrich, St Louis, MO, USA); anti-Lotus Tetragonolobus Lectin (VECTOR Laboratories, Burlingame, CA, USA); E-cadherin (Cell Signaling Technology); anti- α -tubulin, as a loading control, from Calbiochem (San Diego, CA, USA).

Animal Preparation and Procedure

All experimental procedures were performed in accordance with the guidelines of the Animal Research Committee of Tokushima University Graduate School, and protocols were approved by the Institutional Review Board for animal protection. Eight-week-old C57BL/6J mice were obtained from Nippon CLEA (Tokyo, Japan) and they were maintained with free access to water and food (Type NMF; Oriental Yeast, Tokyo, Japan). The unilateral ureteral obstruction (UUO) procedure was previously described in detail.¹⁵ Our mouse model of chronic iron treatment was produced as previously described.¹² Briefly, intraperitoneal SFO (2 mg in a volume of 200 μ l per 25 g mouse) or the same volume of vehicle was administered for five consecutive days. The mice were killed 24 h after the last iron treatment with an intraperitoneal injection of over-dose pentobarbital, and the kidney was removed and stored at -80 °C until use.

Induction of Anemia by Phlebotomy

Phlebotomy was performed for two consecutive days. Briefly, after anesthesia, approximately 400 μ l blood was removed via retroorbital bleeding and was replaced by the same volume of

sterile normal saline by a subcutaneous injection. Then, the mice were administered the vehicle or SFO via an intraperitoneal injection and were placed on a heating pad until full recovery. The mice were killed 24 h after the last phlebotomy.

Cell Culture

Although renal EPO-producing cells are suggested to be derived from tubular interstitial cells such as fibroblasts^{16,17} or pericytes,¹⁸ there are no cell lines established. Therefore, HepG2 cells, a human hepatoma cell line, have been used as EPO-producing cells in *in vitro* experiments.^{19–21} Similarly, we used HepG2 cells to investigate the mechanism of iron on EPO regulation in this study. HepG2 cell was purchased from the Japanese Collection of Research Bioresources (Osaka, Japan). The cells were cultured in Dulbecco's Modified Eagle's Medium (DMEM; Wako Pure Chemical Industries, Osaka, Japan) according to the protocol. For each experiment, the cells at passage 5–8 were used. The cells were grown to confluence, then transferred to serum-free medium before the start of the experiments. In some experiments, the cells were pretreated with 100 μ M CoCl₂, 200 μ M DMOG, and 100 μ M tempol for 1 h before stimulation with SFO.

RNA Extraction and Evaluation of mRNA Expression Levels

RNA extraction, cDNA synthesis, and quantitative RT-PCR methods have been previously described.¹⁵ Briefly, the tissues or cells were homogenized in RNeasy reagent (Takara Bio, Otsu, Japan). RNA extraction and cDNA synthesis were performed according to the manufacturer's instructions (PrimeScript RT reagent Kit with gDNA Eraser (Perfect Real Time), Takara Bio). Quantitative RT-PCR was performed using the CFX Connect Real-Time PCR Detection System (Bio-Rad Laboratories, Hercules, CA, USA) with THUNDERBIRD SYBR qPCR Mix (TOYOBO CO., LTD., Osaka, Japan). The expression levels of all target genes were normalized using *36B4* as an internal control.¹⁵ The primer sets used are noted in Table 1.

Protein Extraction and Western Blot Analysis

Protein preparation and western blotting were performed as previously described.¹⁵ Briefly, the tissues or cell samples were homogenized and sonicated, and then proteins were extracted. The extracted proteins were boiled for 5 min in Laemmli sample buffer and separated using SDS-PAGE. The proteins were transferred to a polyvinylidene fluoride (PVDF) membrane and the membrane was blocked for 1 h at room temperature. Next, the membrane was incubated individually with each primary antibody overnight at 4 °C, followed by incubation for 1 h with the secondary antibody. Immunoreactive bands were detected using a chemiluminescence reagent and visualized by exposure onto an X-ray film or by C-DiGit chemiluminescent scanner (LI-COR C-DiGit Blot Scanner, Lincoln, NE, USA). Densitometry of the visualized bands was quantified using Image J 1.38 \times software.

Table 1 Sequence of the primers for real-time PCR

Target gene	Forward (5'-3')	Reverse (5'-3')
Mouse <i>EPO</i>	ATGTCGCCTCCAGATACCAC	CCTCTCCCGTGACAGCTTC
Mouse <i>HIF-2α</i>	CTAAGTGGCCTGTGGGTGAT	CGAAGTCCTTTGCAGACCTC
Mouse <i>HIF-1α</i>	TCAAGTCAGCAACGTGGAAG	TATCGAGGCTGTGTCGACTG
Mouse <i>VEGF</i>	CAGGCTGCTGTAAACGATGAA	GCATTACATCTGCTGTGCT
Mouse <i>PHD3</i>	CAGGTTATGTTCCCATGTG	TGGCGTCCCAATTCTTATTC
Mouse <i>PGK1</i>	GTCGTGATGAGGGTGGACTT	TTTGATGCTTGAACAGCAG
Human <i>EPO</i>	TCCGAACAATCACTGCTGA	CCTCCCCTGTGTSCSGCTTC
Human <i>HIF-2α</i>	TGCTGGATTGGTTCACACAT	GGGCCAGGTGAAAGTCTACA
Human <i>HIF-1α</i>	TGCTCATCAGTTGCCACTTC	TCCTCACACGCAATAGCTG
Human <i>VEGF</i>	AAGGAGGAGGGCAGAATCAT	CACACAGGATGGCTTGAAGA
Human <i>PHD3</i>	AGATCGTAGGAACCCACACG	TTCTGCCCTTCTTCAGCAT
Human <i>PGK1</i>	GAAGTGGAGAAAGCCTGTGC	GCATCTTTCCCTTCCTTC
36B4	GCTCCAAGCAGATGCAGCA	CCGGATGTGAGGCAGCAG

Immunohistochemistry in the Kidney

The extracted kidney tissues were embedded in OCT compound (Tissue-Tek, SAKURA Finetek, Tokyo, Japan) and frozen in liquid nitrogen-cold isopentane. Samples were cut into 8- μ m sections, dried, and fixed in 4% paraformaldehyde for 10 min. After blocking, the tissue sections were incubated with primary antibodies at 4 °C overnight. Antibody distribution was visualized using immunofluorescence (Alexa fluor; Life Technology, Tokyo, Japan). The sections incubated without primary antibody were used as negative controls.

Measurement of Tissue Iron Content

Tissue iron content was measured using an iron assay kit according to the manufacturer's instructions (Metallo assay, Metallogenics, Chiba, Japan) as described previously.^{15,22} Briefly, the extracted kidney tissues were weighed and homogenized in cell lysis buffer. Non-centrifuged crude lysates were additionally sonicated, then added and mixed with 6 N hydrochloric acid to a final concentration of 0.05 M at room temperature for 30 min. After centrifugation, the supernatants were used for iron measurement. Tissue iron concentration was corrected using tissue weight and expressed as μ g Fe per gram of wet tissue.

Cell Viability Assay

Cell viability was accessed using CellTiter 96 AQueous nonradioactive cell proliferation assay kit (Promega KK, Tokyo, Japan).²³ Briefly, HepG2 cells were seeded in 96-well plates at 1×10^4 cells per well and incubated for 24 h. Subsequently, various concentrations of SFO were added for 24 h and the impact of SFO on cell viability was assessed 1 h after the addition of MTS reagent by measuring absorbance at

490 nm with a plate reader (iMARK microplate reader, Bio-Rad Laboratories).

Detection of Labile Ferrous Iron

We used RhoNox-1 to detect intracellular labile ferrous iron. RhoNox-1 was kindly provided from Dr Tasuku Hirayama and Professor Hideko Nagasawa.²⁴ In brief, an unfixed frozen section of the kidney was washed with Hank's Balanced Salt Solution (HBSS) three times and incubated with RhoNox-1 in HBSS (5 μ M) in a dark, humidified container at room temperature for 30 min. After washing with HBSS three times, the section was covered with a small drop of the mounting medium, and observed using fluorescence microscopy. In some experiments, the frozen sections were fixed in 10% neutral formaldehyde for 1 min, washed with HBSS, and incubated with RhoNox-1.²⁵ Then, the sections were incubated with the primary antibody at 4 °C overnight in a dark humidified container. Lectin and E-cadherin were used as a marker of the proximal and distal tubules, respectively. In HepG2 cells, the cells were seeded in a 24-well culture plate or a black 96-well microplate. HepG2 was stimulated with SFO for 1 h and then loaded with 5 μ M RhoNox-1 in HBSS at 37 °C for 30 min. After washing, ferrous iron was observed using fluorescence microscopy or quantitatively measured at 530 and 575 nm for RhoNox-1 using a fluorescence microplate reader (Varioskan Flash, Thermo Fisher Scientific, Waltham, MA, USA).

In Situ Oxidative Stress Detection in Kidney Tissue

Detection of superoxide production in the kidney was evaluated by dihydroethidium (DHE) staining method as described previously.²² Briefly, non-fixed frozen tissue sections were incubated with DHE in PBS (10 μ M) in a dark, humidified container at room temperature for 30 min and then observed using fluorescence microscopy.

Intracellular Reactive Oxidative Species Detection

Intracellular reactive oxidative species (ROS) were detected using 2',7'-dichlorofluorescein diacetate (DCFH-DA; Sigma-Aldrich, St Louis, MO, USA). HepG2 was stimulated with SFO for 1 h and then loaded with 10 μ M DCFH-DA at 37 °C for 30 min. After washing, ROS production was observed using fluorescence microscopy or quantitatively measured at 488 and 532 nm for DCFH-DA using a microplate reader (FilterMax F3 Multi-Mode Microplate Readers, Molecular Devices, Sunnyvale, CA, USA).

Chromatin Immunoprecipitation

Chromatin immunoprecipitation (ChIP) was performed to determine the interaction between the HIF-2 α protein and *Epo* gene promoter containing the hypoxia response element (HRE). Briefly, the HepG2 cells treated with vehicle or SFO, and with or without tempol were crosslinked with formaldehyde at a final concentration of 1.0% for 10 min, then added to 2.5 mM glycine to stop the crosslinking reaction. Then,

cells were collected, incubated with cell lysis buffer, and the nuclear fraction was extracted. After sonication and centrifugation, the supernatant fraction was co-immunoprecipitated with HIF-2 α protein using agarose beads (Protein A/G plus-Agarose, Santa Cruz Biotechnology). The beads were washed and incubated at 65 °C in elution buffer to reverse the cross-links. DNA was purified from the elution buffer and used for PCR. The primer sequence for the HRE-containing region of the human *EPO* promoter was used as shown previously.²⁶ The primer sequences, used to amplify the

HRE-containing region of the human *EPO* promoter were as follows: *EPO* forward primer 5'-TCGTTTTCTGGGAACCTCCA-3', and *EPO* reverse primer 5'-GGAGCCACCTTATTGACCAG-3'.

Hypoxia-Responsive Element Luciferase Reporter Assay

The hypoxia-responsive reporter vector was constructed using three tandem copies of the HRE from the human *EPO* gene subcloned into the secreted luciferase from the marine copepod *Metridia longa* transcription unit

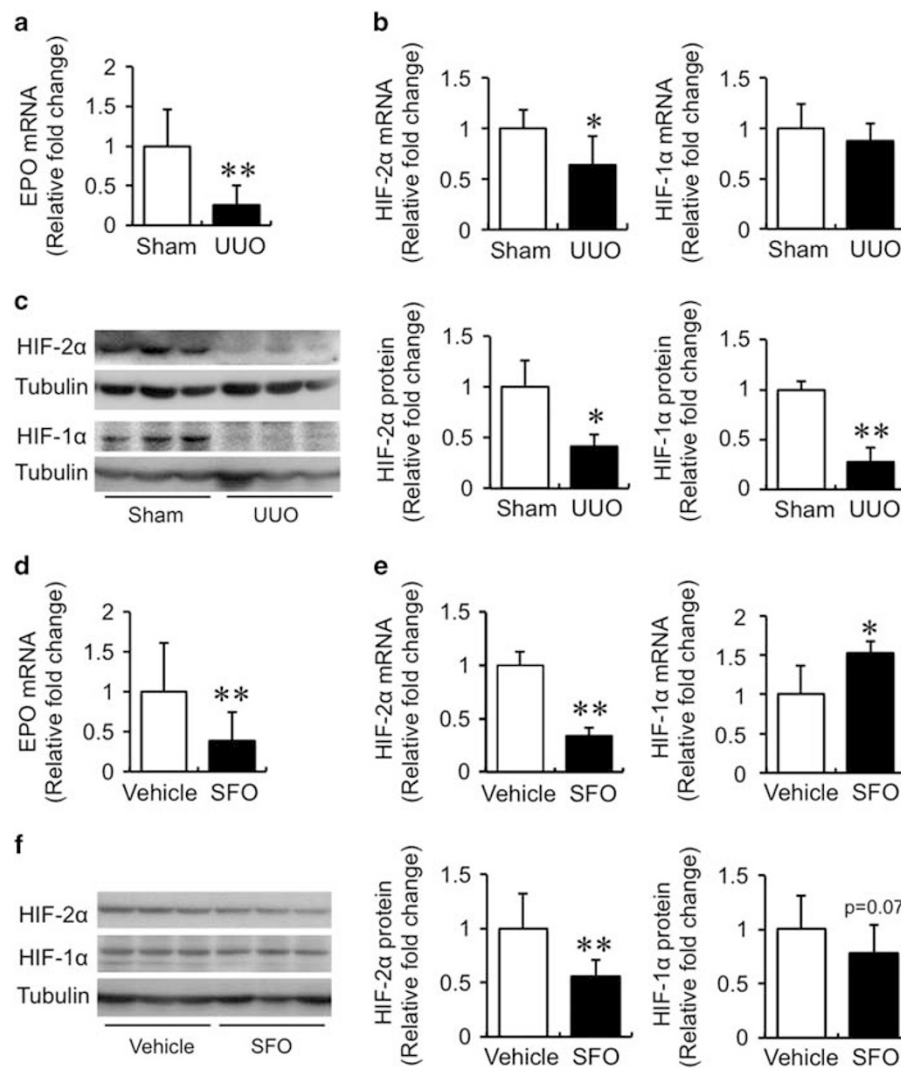


Figure 1 Expression of erythropoietin (EPO) and hypoxia-inducible factors (HIFs) in kidneys with unilateral ureteral obstruction (UUO) and iron treatment. (a) Changes in *EPO* mRNA expression from kidney of sham-operated or UUO mice at day 7. Quantitative real-time reverse transcriptase-polymerase chain reaction (qRT-PCR) analysis of *EPO* mRNA expression. The values are expressed as means \pm s.d. ** P < 0.01 vs sham operation; n = 12 in each group. (b) qRT-PCR analysis of HIF-2 α and HIF-1 α mRNA expression. The values are expressed as means \pm s.d. ** P < 0.05 vs sham operation; n = 12 in each group. (c) Left panels; representative figures of HIF-2 α and HIF-1 α protein expression. The values are expressed as means \pm s.d. * P < 0.05, ** P < 0.01 vs sham operation; n = 3 in each group. (d) Changes in *EPO* mRNA expression from kidney of vehicle- or SFO-treated UUO mice. qRT-PCR analysis of *EPO* mRNA expression. The values are expressed as means \pm s.d. ** P < 0.01 vs vehicle; n = 11–13. (e) qRT-PCR analysis of HIF-2 α and HIF-1 α mRNA expression. The values are expressed as means \pm s.d. * P < 0.05, ** P < 0.01 vs vehicle treatment; n = 11–13 in each group. (f) Left panels; representative figures of HIF-2 α and HIF-1 α protein expression. Right panel: semi-quantitative analysis of densitometry for HIF-2 α and HIF-1 α protein expression. The values are expressed as means \pm s.d. ** P < 0.01 vs vehicle treatment; n = 12 in each group.

(pCre-MetLuc2-Reporter plasmid vector, Takara Bio, Shiga, Japan). One hundred nanograms pCre-MetLuc-HRE plasmid vector and 10 ng pSEAP2-Control plasmid vector (Takara Bio) were co-transfected in 1×10^4 HepG2 cells using Lipofectamine 2000 (Thermo Fisher Scientific) in a 96-well culture plate. The transfected cells were exposed to the vehicle or SFO for 24 h and then the cell culture medium was harvested and both luciferase and alkaline phosphatase (ALP) activities were measured using Secreted Luciferase Reporter Assay (Takara Bio) and SEAP Reporter Gene Assay (Sigma-Aldrich Japan K.K., Tokyo, Japan), respectively, according to the manufacturer's instructions. To normalize the transfection efficiency, the RLU of the luciferase chemiluminescence unit was divided by that of the ALP chemiluminescence unit.

Measurement of Plasma EPO Concentration

Plasma EPO concentration was determined by using an ELISA kit, according to the manufacturer's instructions (Mouse Erythropoietin Quantikine ELISA Kit, R&D systems, Minneapolis, MN, USA).

Statistical Analysis

The data are presented as mean \pm s.d. An unpaired, two-tailed Student's *t*-test was used for comparison between the two groups. For comparisons between more than two groups, the statistical significance of each difference was evaluated by *post hoc* test using Dunnett's method or Tukey-Kramer's method. Statistical significance was indicated by $P < 0.05$.

RESULTS

EPO Expression and Iron Content in The Kidney with UUO surgery

EPO mRNA levels are drastically reduced in kidneys with UUO surgery.¹⁷ Similarly, *EPO* mRNA expression was decreased in the kidney at 7 days after UUO surgery compared with sham operation (Figure 1a). We have already demonstrated that renal iron content was significantly augmented in UUO-induced fibrotic kidney in the previous study.¹⁵

EPO Expression and Iron Content in the Kidney of Iron-Treated Mice

To examine direct action of iron on *EPO* expression, we used mice with SFO treatment. Renal iron content was significantly increased in mice with SFO treatment for consecutive five days compared with vehicle-treated mice (vehicle; $12.0 \pm 3.6 \mu\text{g}$ Fe per gram of wet tissue, SFO; $20.8 \pm 4.2 \mu\text{g}$ Fe per gram of wet tissue, $n = 3$, $P < 0.05$). *EPO* mRNA expression was decreased in the kidney of SFO-treated mice compared with vehicle-treated mice (Figure 1d). Similarly, the plasma EPO concentration was also suppressed in SFO-treated mice (Table 4). There were no significant differences in hematological parameters of red blood cells between vehicle- and SFO-treated mice (Table 2).

Table 2 Hematological characteristics

	RBC ($\times 10^4/\mu\text{l}$)	Hb (g/dl)	Ht (%)	WBC (/ μl)	Platelet ($\times 10^4/\mu\text{l}$)
Vehicle	870 ± 50	13.2 ± 0.9	40.7 ± 2.2	4575 ± 340	58.4 ± 3.2
SFO	828 ± 54	12.6 ± 0.9	38.9 ± 2.7	$7623 \pm 684^{**}$	$45.6 \pm 7.9^*$

Data are means \pm s.d; $n = 4$; $*P < 0.05$, $**P < 0.01$ vs vehicle-treated mice.

HIF-2 α Expression in the Kidney with UUO and Iron-Treated Mice

HIF-2 α is an important regulator of *EPO* expression in the kidney²⁷ and liver.²⁶ HIF-2 α expression was diminished in the kidneys with UUO and iron treatment compared with the kidneys with sham or vehicle treatment (Figure 1c and f). These findings suggest that iron accumulation suppresses renal *EPO* expression through the inhibition of HIF-2 α . In contrast, HIF-1 α mRNA was not changed and HIF-1 α protein was decreased in the kidney of UUO mice (Figure 1b and c), whereas HIF-1 α mRNA was elevated and HIF-1 α protein tended to decrease in the kidney of SFO-treated mice (Figure 1e and f).

SFO Action on Transition of Fibroblast to Myofibroblast in Kidneys

EPO production occurs in fibroblasts, and loss of *EPO* production occurs during the transition of fibroblast to myofibroblast in the course of renal fibrosis progression.^{16,17} The fibroblast to myofibroblast transition has an important role in the process of renal fibrosis.²⁸ Therefore, we checked whether iron was involved in the fibroblast to myofibroblast transition-dependent loss of *EPO* production. No apparent parenchymal damages were seen in the kidney of SFO-treated mice compared with vehicle-treated mice (Figure 2a). SFO treatment augmented the expression of PDGF-R β and α -SMA proteins in the kidney, compared with vehicle treatment (Figure 2b and c). Immunohistochemical analysis showed that PDGF-R β expression was increased in the renal interstitium of SFO-treated kidneys. The α -SMA expression also increased in the renal interstitium of SFO-treated kidneys. In contrast, it was almost completely localized in vessels in vehicle-treated kidneys. Moreover, PDGF-R β and α -SMA expression were colocalized in the renal interstitium of SFO-treated kidneys (Figure 2d). These results suggest that iron-induced *EPO* reduction occurs due to an induction of renal fibrotic change and the myofibroblast transition.

The Effect of SFO on *EPO* mRNA Expression in HepG2 Cells

First, we performed the MTS cell proliferation assay to determine the effect of SFO on the viability of HepG2 cells. SFO had no effect of cellular viability at 50, 100, and 200 $\mu\text{g}/\text{ml}$ but significantly reduced cell viability at 1000 $\mu\text{g}/\text{ml}$. This result indicates that high concentrations of SFO are toxic for HepG2

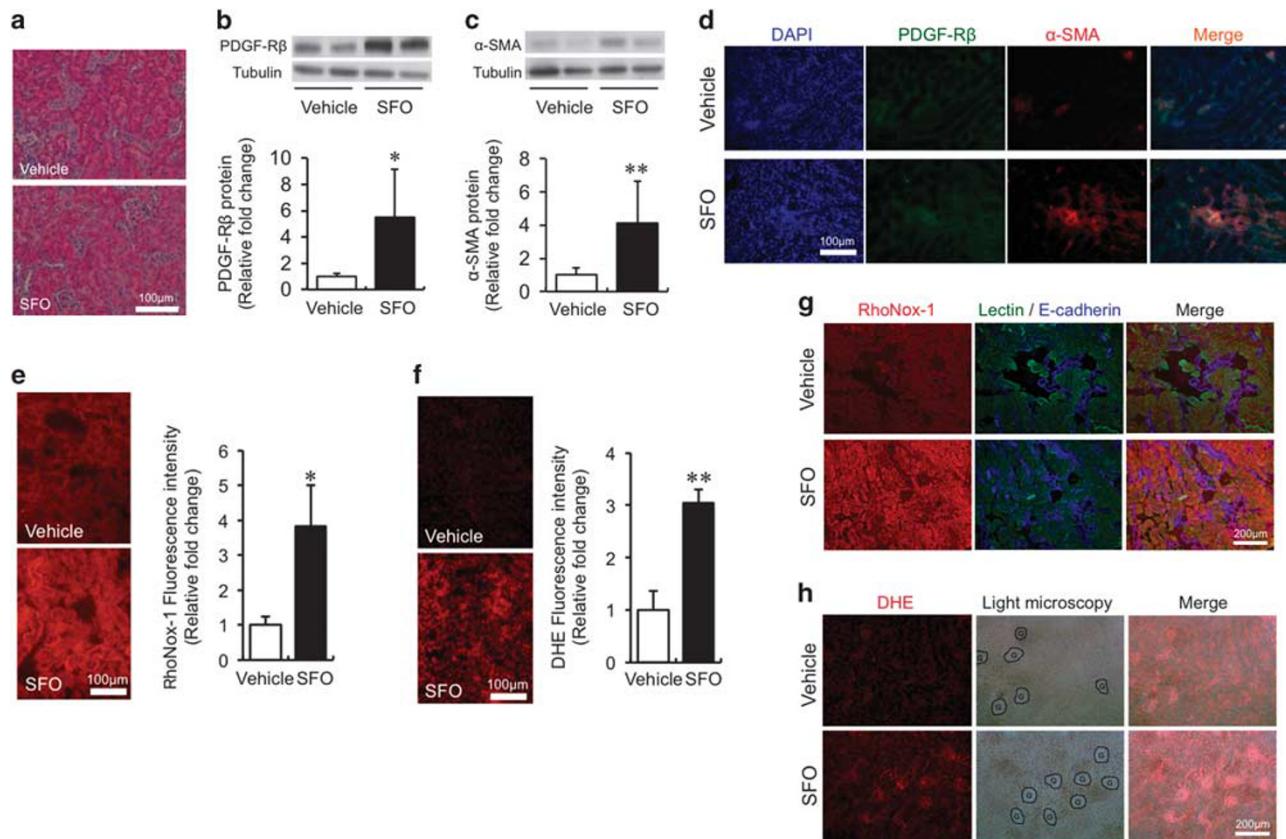


Figure 2 (a) Representative hematoxylin and eosin staining of the kidney section. (b) Western blot analysis showing the effects of iron on PDGF-R β and α -SMA expression in kidney. Upper panels; representative figures of PDGF-R β from kidney with vehicle or SFO treatment. Lower panel: semi-quantitative analysis of densitometry for PDGF-R β expression. The values are expressed as means \pm s.d. * P < 0.05 vs vehicle treatment; n = 8 in each group. (c) Upper panels; representative figures of α -SMA from the kidney with vehicle or SFO treatment. Lower panel: semi-quantitative analysis of densitometry for α -SMA expression. The values are expressed as means \pm s.d. ** P < 0.01 vs vehicle treatment; n = 4 in each group. (d) Iron-induced transition from fibroblast to myofibroblast in kidney. Representative immunohistochemistry of DAPI (blue), PDGF-R β (green), and α -SMA (red) staining. (e) SFO-increased labile ferrous iron in the kidney. Left panels; representative figures of RhoNox-1 staining in the kidney with or without SFO treatment. Right panel: semi-quantitative analysis of fluorescence intensity. The values are expressed as means \pm s.d. * P < 0.05 vs vehicle treatment; n = 4 in each group. (f) Iron-induced oxidative stress production in the kidney. Left panels; representative figures of dihydroethidium (DHE) staining in kidney with or without SFO treatment. Right panel: semi-quantitative analysis of fluorescence intensity. The values are expressed as means \pm s.d. ** P < 0.01 vs vehicle treatment; n = 3 in each group. (g) Fluorescence image of lectin (green), E-cadherin (blue), RhoNox-1 (red), and merged image of the same field of the kidney section. (h) Fluorescence and light microscope images of DHE staining, and merged image of the same field of the kidney section. G, glomeruli.

cells (Figure 3a). Therefore, we used SFO at concentrations of 200 μ g/ml and below in further studies. To examine the effect of SFO on EPO regulation, we examined EPO mRNA expression after treatment with various concentration of SFO. As shown in Figure 3b, SFO significantly reduced EPO mRNA expression in a dose-dependent manner. HIF-2 α mRNA and protein levels were also reduced by SFO treatment in HepG2 cells (Figure 3c and d). Similarly, the expression of HIF-1 α at the mRNA and protein levels decreased in HepG2 cells (Figure 3c and d). The results of these *in vitro* experiments are consistent with *in vivo* results demonstrating the effect of SFO on EPO and HIF-2 α expression in the kidney.

The Suppressive Effects of SFO on CoCl₂ or DMOG-induced EPO and HIF-2 α Upregulation

We examined the effects of SFO on EPO and HIF-2 α expression under hypoxic conditions, using cobalt chloride to

mimic conditions of hypoxia induction. EPO mRNA and HIF-2 α protein expression were increased by cobalt chloride treatment. The hypoxia-induced increases in EPO mRNA and HIF-2 α protein expression were suppressed by combining SFO and cobalt chloride treatments (Figure 3e and f). DMOG is a prolyl hydroxylase inhibitor drug, and is also used for the induction of HIF expression. As observed with cobalt chloride, DMOG treatment increased EPO mRNA and HIF-2 α protein expression, and these increases were inhibited by concomitant SFO treatment (Figure 3g and h). Cobalt chloride- or DMOG-induced HIF-1 α protein expression was also decreased by concomitant SFO treatment (Figure 3f and h).

SFO Treatment Induced Oxidative Stress

Excess iron causes oxidative stress by producing hydroxyl radicals via the Fenton reaction.²⁹ SFO treatment actually

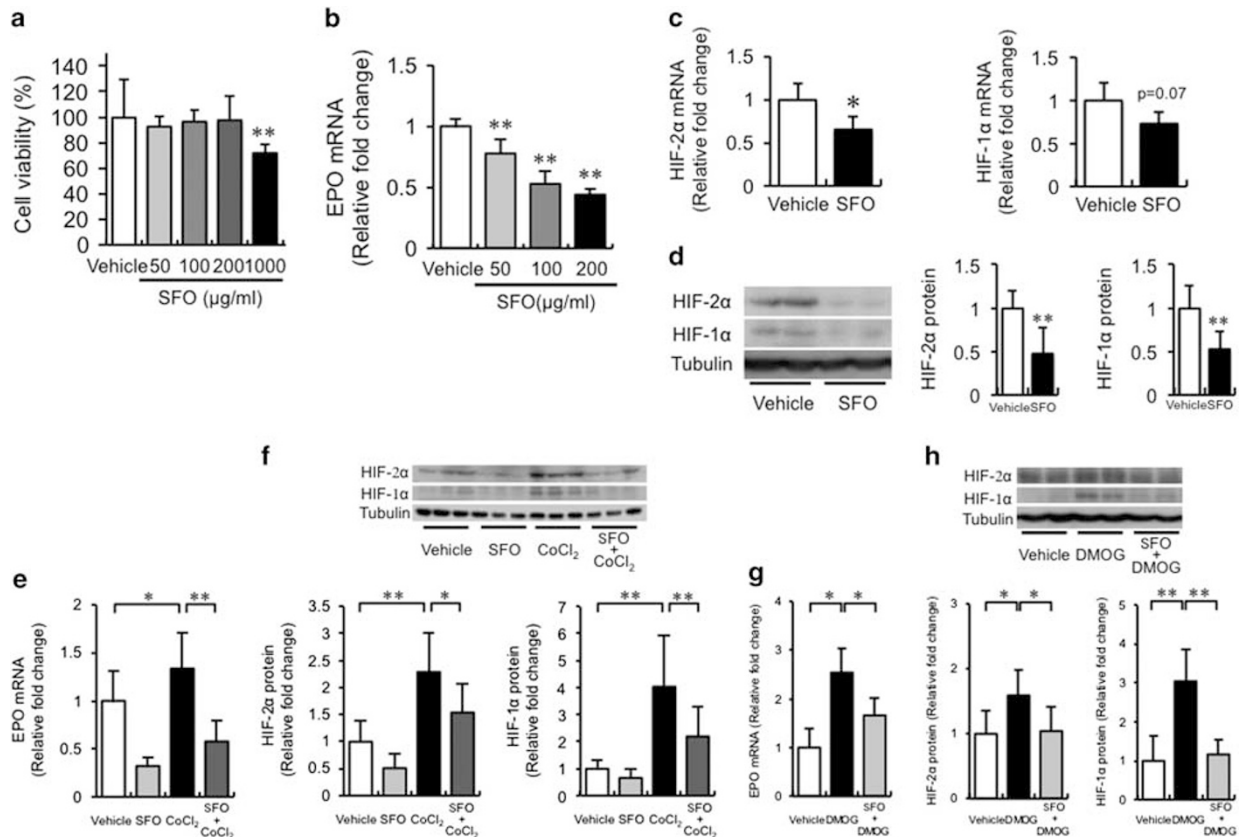


Figure 3 The effect of iron on EPO and HIFs expression in HepG2 cells. (a) HepG2 cell viability was significantly decreased only by 1000 µg/ml SFO treatment. The values are expressed as means ± s.d. ** $P < 0.01$ vs vehicle treatment; $n = 8$ in each group. (b) Impact of SFO on *EPO* mRNA expression and dose-dependency in HepG2 cells. The values are expressed as means ± s.d. ** $P < 0.01$ vs vehicle treatment; $n = 4$ in each group. SFO action on HIFs expression in HepG2 cells. (c) Quantitative analysis of HIF-2α and HIF-1α mRNA expression. The values are expressed as means ± s.d. * $P < 0.05$ vs vehicle treatment; $n = 6$. (d) Left panels; representative figures of HIF-2α, HIF-1α, and tubulin with vehicle or SFO treatment. Right panel: semi-quantitative analysis of densitometry for HIF-2α and HIF-1α protein expression. The values are expressed as means ± s.d. ** $P < 0.01$ vs vehicle treatment; $n = 6$ in each group. (e) Suppressive effect of SFO on cobalt chloride-induced *EPO* mRNA upregulation in HepG2 cells. The values are expressed as means ± s.d. * $P < 0.05$, ** $P < 0.01$ vs vehicle treatment; $n = 8$ in each group. (f) SFO suppressive action on cobalt chloride-induced upregulation of HIF-2α and HIF-1α protein expression in HepG2 cells. Upper panels; representative figures of HIF-2α, HIF-1α and tubulin. Lower panel: semi-quantitative analysis of densitometry for HIF-2α and HIF-1α expression. Values are expressed as means ± s.d. * $P < 0.05$, ** $P < 0.01$ vs vehicle treatment; $n = 9$ in each group. (g) Inhibitory effect of SFO on DMOG-induced *EPO* mRNA upregulation in HepG2 cells. The values are expressed as means ± s.d. * $P < 0.05$ vs vehicle treatment; $n = 4$ in each group. (h) SFO inhibitory effect on DMOG-induced upregulation of HIF-2α and HIF-1α expression in HepG2 cells. Upper panels; representative figures of HIF-2α, HIF-1α and tubulin. Lower panel: semi-quantitative analysis of densitometry for HIF-2α and HIF-1α expression. The values are expressed as means ± s.d. * $P < 0.05$, ** $P < 0.01$ vs vehicle treatment; $n = 8$ in each group.

increased labile ferrous iron mainly in both the proximal and distal tubule of the kidney (Figure 2e and g), and HepG2 cells (Figure 4a), suggesting to iron-induced oxidative stress consequent to Fenton reaction. Here, we showed that SFO induced oxidative stress in the kidney (Figure 2f). SFO-induced oxidative stress seemed to be dominantly localized in the glomeruli and a part of the proximal tubule (Figure 2h). SFO-induced oxidative stress was also observed in HepG2 cells (Figure 4b), and it was diminished by the antioxidant compound, tempol (Figure 4c). Iron content was elevated with SFO treatment, which did not change following tempol treatment (vehicle; 424 ± 460 ng Fe per gram protein, SFO; 9297 ± 685 ng Fe per gram protein, SFO+tempol; 9597 ± 880 ng Fe per gram protein). The

suppressive effects of SFO on *EPO* mRNA and HIF-2α protein expression, but not *HIF-2α* mRNA, were prevented by tempol treatment (Figure 4d–f). SFO-induced reduction in HIF-1α protein was restored by tempol treatment (Figure 4f). These findings indicate that SFO-mediated suppression of *EPO* and HIF-2α expression occurs via SFO-induced oxidative stress.

SFO Suppressed the Interaction Between the HIF-2α Protein and Epo-HRE Containing Promoter

We performed ChIP to examine the interaction between the HIF-2α protein and *Epo*-HRE containing promoter region. As shown in Figure 4g, SFO treatment reduced HIF-2α binding to the *Epo* promoter. The suppressive action of SFO

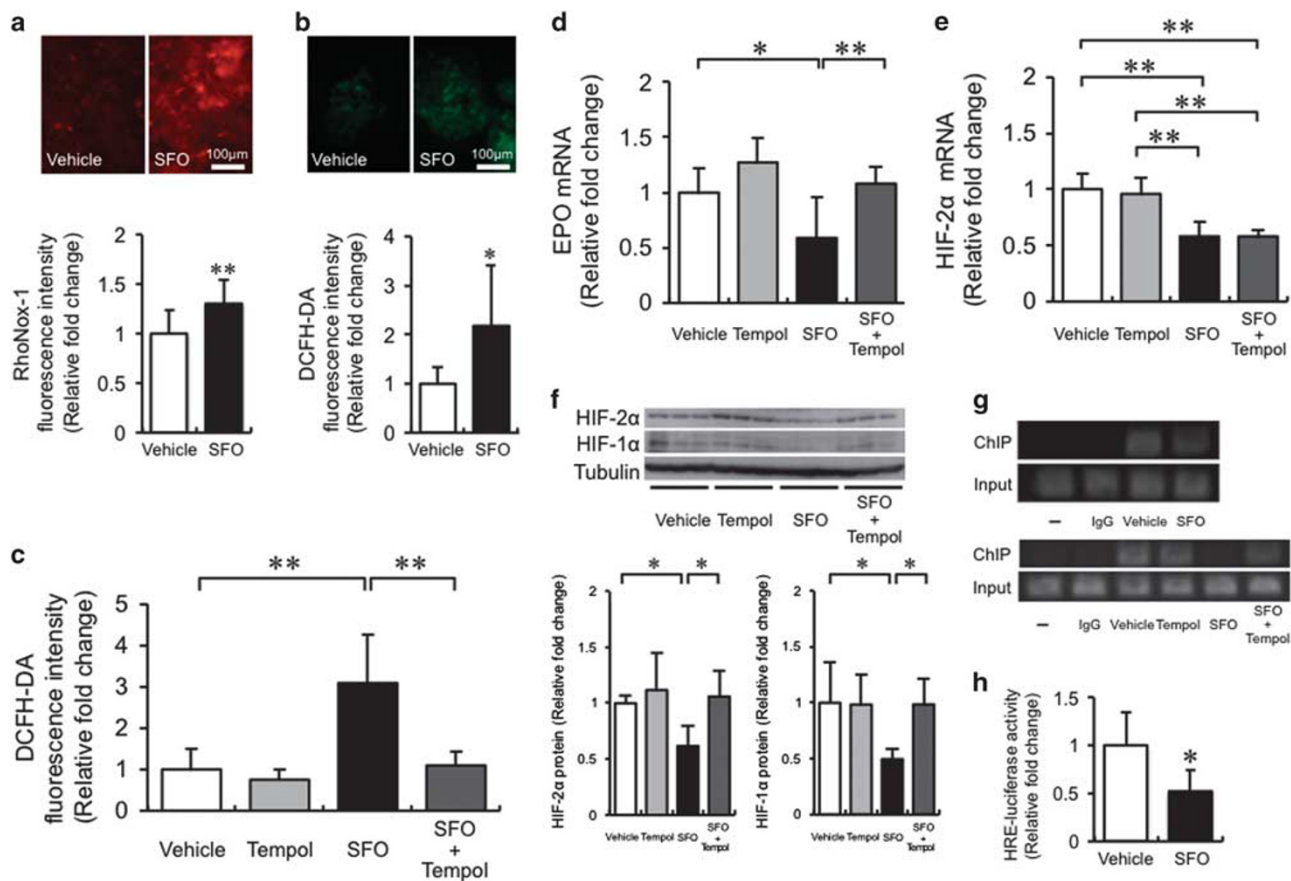


Figure 4 Involvement of oxidative stress in iron-induced downregulation of *EPO* and HIFs expression in HepG2 cells. (a) Upper panels; representative figures of RhoNox-1 staining in HepG2 cells with or without SFO. Lower panel: quantitative analysis of fluorescence intensity measured by microplate reader. The values are expressed as means \pm s.d. $**P < 0.01$ vs vehicle treatment; $n = 8$ in each group. (b) Upper panels; representative figures of DCFH-DA staining in HepG2 cells with or without SFO. Lower panel: quantitative analysis of fluorescence intensity measured by microplate reader. The values are expressed as means \pm s.d. $*P < 0.05$ vs vehicle treatment; $n = 16$ in each group. (c) Effect of antioxidant agent on SFO-induced oxidative stress. Quantitative analysis of DCFH-DA fluorescence intensity measured by microplate reader. The values are expressed as means \pm s.d. $**P < 0.01$; $n = 16$ in each group. (d) Restorative effect of tempol on SFO-induced *EPO* mRNA downregulation in HepG2 cells. The values are expressed as means \pm s.d. $*P < 0.05$, $**P < 0.01$ vs vehicle treatment; $n = 8$ in each group. (e) Tempol has no effect on SFO-induced HIF-2 α mRNA downregulation in HepG2 cells. The values are expressed as means \pm s.d. $**P < 0.01$ vs vehicle treatment; $n = 8$ in each group. (f) Restorative effect of tempol on iron-induced downregulation of HIF-2 α and HIF-1 α expression in HepG2 cells. Upper panel: representative figures of HIF-2 α , HIF-1 α , and tubulin. Lower panel: semi-quantitative analysis of densitometry for HIF-2 α and HIF-1 α expression. The values are expressed as means \pm s.d. $*P < 0.05$ vs vehicle treatment; $n = 6$ in each group. (g) ChIP analysis of HIF-2 α protein and the *Epo* HRE containing promoter interaction in HepG2 cells. Co-precipitated DNA fragments were detected by PCR using primers spanning the *Epo* HRE region. (h) SFO suppressed HRE-luciferase activity in HepG2 cells. The values are expressed as means \pm s.d. $*P < 0.05$ vs vehicle treatment; $n = 6$ in each group.

on the HIF-2 α and *Epo* gene promoter interaction was restored by tempol treatment. These results suggest that SFO-induced *EPO* downregulation was due to the inactivation of HIF-2 α binding to the *Epo*-HRE containing promoter region.

The Promoter Activity of HRE was Inhibited by SFO Treatment in HepG2 Cells

We also examined the effect of SFO on HRE promoter activity by luciferase assay. As shown in Figure 4h, SFO diminished the promoter activity of HRE by 50%, indicating the inhibitory action of SFO on *Epo* through transcriptional inactivity of HIF.

Effect of SFO on HIF-regulated genes

HIF is a well-known transcriptional regulator for many genes. In addition to *Epo*, we assessed several HIF-regulated genes, such as *Vegf*, *Phd3*, and *Pgk1*. In the *in vivo* studies, SFO treatment elevated mRNA expression of these three genes (Figure 5a). However, only *Phd3* mRNA expression was augmented by SFO treatment in HepG2 cells (Figure 5b). PHD3 has a crucial role in the regulation of HIF-2,³⁰ indicating the involvement of iron in HIF-2 α regulation.

Inhibitory Effect of SFO on Anemia-Induced EPO upregulation

Finally, we examined whether SFO treatment suppresses anemia-induced EPO upregulation by using mice with

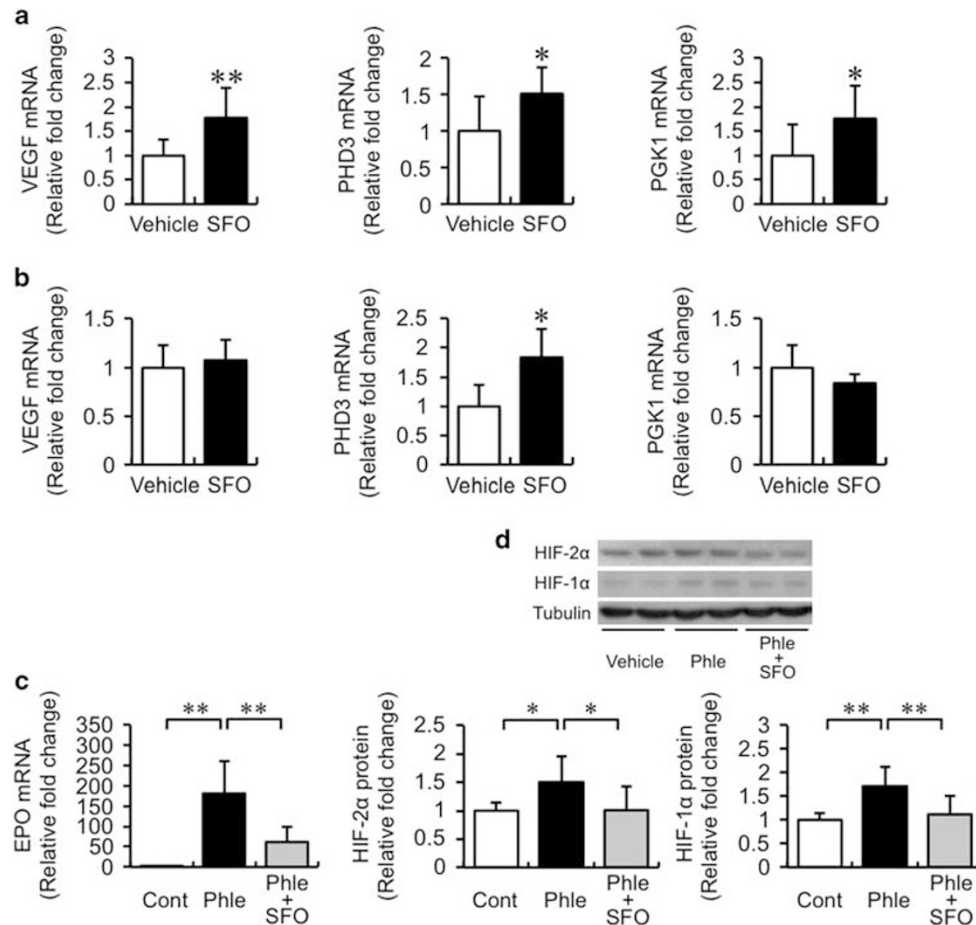


Figure 5 (a) Changes in *VEGF*, *PHD3*, and *PGK1* mRNA expression in the kidney of vehicle- or SFO-treated mice. The values are expressed as means \pm s.d. * P < 0.05, ** P < 0.01 vs vehicle; n = 11–13 in each group. (b) The effect of SFO on *VEGF*, *PHD3*, and *PGK1* mRNA expression in HepG2 cells. The values are expressed as means \pm s.d. * P < 0.05 vs vehicle; n = 4 in each group. Effects of SFO on (c) *EPO* and (d) HIFs in mice with phlebotomy-induced anemia. The values are expressed as means \pm s.d. * P < 0.05, ** P < 0.01 vs vehicle; n = 7 in each group.

Table 3 Hematological characteristics

	RBC ($\times 10^4/\mu\text{l}$)	Hb (g/dl)	Ht (%)	WBC ($/\mu\text{l}$)	Platelet ($\times 10^4/\mu\text{l}$)
Control	897 \pm 39	13.6 \pm 0.6	40.7 \pm 1.7	4367 \pm 2084	54.1 \pm 3.1
Phlebotomy	469 \pm 87**	7.4 \pm 1.3**	22.4 \pm 3.6**	3766 \pm 1666	54.1 \pm 14.7
Phlebotomy +SFO	432 \pm 14**	6.7 \pm 0.4**	20.5 \pm 0.3**	4600 \pm 985	31.1 \pm 19.2

Data are means \pm s.d.; n = 3; ** P < 0.01 vs control mice.

phlebotomy-induced anemia. Phlebotomy-induced anemia in mice, and no differences in hematological parameters were observed in these mice regardless of SFO treatment (Table 3). As shown in Figure 5c and Table 4, anemia induced an increase in renal *Epo* mRNA expression as well as plasma *EPO* concentration, were suppressed by SFO treatment. Moreover, anemia-induced HIF-2 α expression

was also inhibited in SFO-treated mice with phlebotomy (Figure 5d).

DISCUSSION

In CKD, patients with renal anemia are commonly administered parenteral iron supplementation. However, iron treatment itself has adverse effects on various tissues through iron-related oxidative stress production. In the present study, we found that parenteral iron treatment reduced *EPO* mRNA and HIF-2 α protein expression in the mouse kidney. Notably, iron treatment augmented oxidative stress production in both *in vivo* and *in vitro* experiments, and tempol could restore iron-induced reduction of *EPO* and HIF-2 α expression in HepG2 cells. Moreover, iron suppressed HIF-2 α binding to the *Epo*-HRE containing promoter, which was ameliorated by tempol. These results suggest that iron reduces *EPO* expression through HIF-2 α inactivation via oxidative stress production.

Renal fibrosis is an important factor in the progression of CKD leading to end-stage renal disease,³¹ and renal anemia, a

Table 4 Plasma EPO concentration

	Vehicle		SFO
Plasma EPO (pg/ml)	151.5 ± 44.4		103.9 ± 39.4*
	Control	Phlebotomy	Phlebotomy+SFO
Plasma EPO (pg/ml)	148.3 ± 64.8	10731.7 ± 2366.5**	8087.5 ± 2061.3***#

Data are means ± s.d.; *n* = 8–12; **P* < 0.05 vs vehicle-treated mice. Data are means ± s.d.; *n* = 7; ***P* < 0.01 vs control mice, ****P* < 0.05 vs phlebotomy mice.

complication of CKD, develops along with renal fibrosis. The primary cause of renal anemia is inadequate EPO production consequent to loss of renal-EPO-producing cells due to renal fibrosis.¹⁶ The murine UUO model is widely recognized to induce renal fibrosis with reduced EPO expression. Renal EPO expression is drastically reduced at day 1 or later after UUO surgery.¹⁷ In the same murine UUO model, excess iron accumulation is observed in UUO-induced fibrotic kidneys compared with those of sham-operated mice.¹⁵ In addition, we confirmed reduced EPO expression in UUO fibrotic kidneys. Consistent with the association between renal fibrosis and iron accumulation, several studies have shown that iron content is increased in fibrotic kidneys of the angiotensin II-infused rat,³² Dahl salt-sensitive rat,³³ and 5/6 nephrectomized rat.³⁴ We, and others, have shown the anti-fibrotic effect of tissue iron reduction using iron chelators or iron restriction chow on the kidney.^{15,33,34} Here, direct SFO treatment diminished renal EPO expression in the kidney with increased iron content. Therefore, there is a close relationship between iron accumulation and renal fibrosis, resulting in the reduction of EPO expression.

The EPO gene promoter contains a HRE region. HIF promotes EPO transcription through binding to HRE in the EPO promoter.^{26,35} It has been shown that HIF-1 and HIF-2 transcriptionally regulate EPO expression. However, using renal-specific HIF-2α knockout mice, it has been demonstrated that renal EPO expression is predominantly regulated by HIF-2α and not by HIF-1α.³⁶ Using an siRNA approach in Hep3B cells, constituting a hepatoma cell line,³⁷ and mice with conditional hepatic HIF-2α deletion, it has been shown that EPO gene induction is largely dependent on HIF-2, not HIF-1 in the liver.²⁶ Thus, HIF-2α is recognized as a key regulator of EPO expression in both the kidney and liver.

In this study, SFO treatment reduced HIF-2α expression, and HIF-2α protein binding to the EPO promoter region. In addition, SFO-induced HIF-2α inactivation was ameliorated by the antioxidant compound, tempol, indicating the involvement of iron-mediated oxidative stress in HIF-2α regulation. HIFs are generally regulated by post-transcriptional mechanisms that determine the rate of HIF protein degradation,³⁸ and its binding ability.³⁹ Iron itself is shown to antagonize HIF-mediated induction of EPO gene expression induced by cobalt chloride,⁴⁰ and iron

supplementation reduces HIF-1α expression levels even under normoxia in PC3 cells.⁴¹ This is the first study to describe the association between iron and HIF-2α, and to suggest that the preventive action of iron on EPO expression is mediated through a HIF-2α-dependent signaling pathway. Prolyl hydroxylase domain (PHD) also has a crucial role in regulating HIF protein stability, and PHD activity is stimulated by ferric iron, and suppressed by iron chelation.⁴² Correspondingly, DMOG, a PHD inhibitor, induced EPO expression, which was also attenuated by concomitant SFO treatment in HepG2 cells. In addition, PHD3 is known to be a regulator of HIF-2,³⁰ and SFO increased *Phd3* mRNA expression in both the kidney and HepG2 cells, indicating the involvement of iron-induced PHD3 upregulation in HIF-2α reduction. Therefore, SFO-mediated EPO reduction might be involved in the destabilization of HIF-2α protein via the restoration of DMOG-inhibited PHD activity. In contrast to *phd3* mRNA expression, mice with SFO treatment showed increased mRNA expression of *Vegf* and *PGK1* and these genes were not changed in HepG2 cells with SFO treatment. The different expression of HIF-regulated genes induced by iron might be due to tissue or cell from different organ.

Oxidative stress is proposed to participate in regulating the protein stability and transcriptional activity of HIF. H₂O₂ destabilizes HIFs protein under hypoxia.^{43,44} Oxidative stresses such as diamide, *N*-ethylmaleimide, and H₂O₂ also inhibit the DNA binding activity of HIF-1.³⁹ H₂O₂ suppresses hypoxia-induced EPO production in HepG2 cells,⁴⁵ which might be due to oxidative stress-mediated HIF inactivation. Taken together, iron-induced oxidative stress could be responsible for protein stabilization and DNA binding activity of HIF. Moreover, tempol ameliorated SFO-induced inhibition of the HIF-2α–EPO signaling pathway without affecting intracellular iron content. Therefore, concomitant treatment of antioxidant drugs might be effective for reducing the oxidative stress induced by iron supplementation.

HIF proteins are involved in the post-transcriptional regulation of protein expression and activity as well as the regulation of mRNA transcription. Page *et al.*⁴⁶ have shown that HIF-1α expression is increased by angiotensin II via diacylglycerol-sensitive protein kinase C-dependent transcriptional regulation in addition to the ROS-phosphatidylinositol 3-kinase pathway-dependent translational pathway. A recent study has shown that mice deficient in iron-regulatory protein 1 exhibit HIF-2α protein accumulation due to de-repression of HIF-2α mRNA and induce renal EPO expression.⁴⁷ However, inconsistent with the above results, we have shown that SFO treatment decreased HIF-2α mRNA expression in mice kidney and HepG2 cells, indicating that iron negatively regulates HIF-2α expression at the transcriptional level in this study. Moreover, SFO-induced HIF-2α mRNA down-regulation was not changed by tempol treatment, even though SFO-mediated HIF-2α protein downregulation was reversed. This suggests that iron transcriptionally regulates HIF-2α expression independent of iron-mediated oxidative stress, in

addition to the post-transcriptional regulation of protein degradation and the DNA binding activities of HIF-2 α . Further studies are necessary to clarify the mechanism of iron regulation on HIF-2 α activation.

Recent studies demonstrate that renal EPO production cells are derived from fibroblasts, and the transition of fibroblast to myofibroblast is the main cause of renal fibrosis²⁸ and loss of EPO production in CKD.^{16,17} We previously reported that the UUO-induced increase of α -SMA expression in the interstitium was reduced by iron chelation.¹⁵ This indicates that iron participates in the myofibroblast transition during the process of renal fibrosis. Here, we also found that PDGF-R β (a fibroblast marker) and α -SMA (a myofibroblast marker) expression were enhanced, and that PDGF-R β and α -SMA were colocalized in the tubulo-interstitium in kidneys with SFO treatment. These findings suggest that iron promotes renal fibrotic change with transition of fibroblasts to myofibroblasts, in part leading to an iron-induced reduction of EPO expression. In contrast, superoxide, as well as ferrous iron, was not observed in the renal tubulo-interstitium. Therefore, further studies are required to clarify the interaction between fibroblast, oxidative stress, and iron in the kidney.

In the present study, SFO-treated mice showed the reduced plasma EPO concentration and the lower level of RBC, Hb, and Ht compared with vehicle-treated mice, suggesting the decrease of erythropoiesis due to iron-induced reduction of EPO production. On the other hand, WBC counts were elevated by SFO treatment. Intravenous iron treatment induces protein oxidation, which positively correlates to CRP levels in hemodialysis patients,⁴⁸ indicating the association between iron-induced oxidative stress and inflammation. Therefore, iron treatment perhaps causes inflammation as well as oxidative stress, resulting in the increased number of WBC.

In regard to mice model of UUO, HIF-1 α mRNA was not changed and HIF-1 α protein was diminished in UUO kidney at day 7 after surgery in our study. Souma *et al.*¹⁷ demonstrate that HIF-1 α mRNA was increased in UUO kidney at day 2 after surgery. This discrepancy of HIF-1 α expression might be responsible for the different sampling point after UUO induction or the discordance of protein and mRNA expression.

In conclusion, parenteral iron supplementation reduced EPO gene expression via oxidative stress-induced HIF-2 α inactivation. These findings suggest a new potential risk of parenteral iron supplementation and a causative role of therapeutic excess iron in the further deterioration of endogenous erythropoietin production in CKD.

Supplementary Information accompanies the paper on the Laboratory Investigation website (<http://www.laboratoryinvestigation.org>)

ACKNOWLEDGMENTS

This work was partly supported by JSPS KAKENHI Grant (No. 15K01716) and the grant provided The Ichiro Kanehara Foundation to YI. We appreciate the

excellent technical advice by Support Center for Advanced Medical Sciences, Institute of Biomedical Sciences, Tokushima University Graduate School. We thank Editage (www.editage.jp) for English language editing.

DISCLOSURE/CONFLICT OF INTEREST

The authors declare no conflict of interest.

- Collins AJ, Foley RN, Gilbertson DT, *et al.* The state of chronic kidney disease, ESRD, and morbidity and mortality in the first year of dialysis. *Clin J Am Soc Nephrol* 2009;4(Suppl 1):S5–S11.
- Go AS, Chertow GM, Fan D, *et al.* Chronic kidney disease and the risks of death, cardiovascular events, and hospitalization. *N Engl J Med* 2004;351:1296–1305.
- Levey AS. Controlling the epidemic of cardiovascular disease in chronic renal disease: where do we start? *Am J Kidney Dis* 1998;32(5 Suppl 3): S5–S13.
- Astor BC, Muntner P, Levin A, *et al.* Association of kidney function with anemia: the Third National Health and Nutrition Examination Survey (1988–1994). *Arch Intern Med* 2002;162:1401–1408.
- Paganini EP. Overview of anemia associated with chronic renal disease: primary and secondary mechanisms. *Semin Nephrol* 1989;9 (1 Suppl 1):3–8.
- Kdoqi, National Kidney F. KDOQI clinical practice guidelines and clinical practice recommendations for anemia in chronic kidney disease. *Am J Kidney Dis* 2006;47(5 Suppl 3):S11–S145.
- Babitt JL, Lin HY. Mechanisms of anemia in CKD. *J Am Soc Nephrol* 2012;23:1631–1634.
- Nakanishi T, Kuragano T, Nanami M, *et al.* Importance of ferritin for optimizing anemia therapy in chronic kidney disease. *Am J Nephrol* 2010;32:439–446.
- Nakanishi T, Hasuiki Y, Otaki Y, *et al.* Hcpidin: another culprit for complications in patients with chronic kidney disease? *Nephrol Dial Transplant* 2011;26:3092–3100.
- Zhao N, Zhang AS, Enns CA. Iron regulation by hepcidin. *J Clin Invest* 2013;123:2337–2343.
- Rooyackers TM, Stoes ES, Kooistra MP, *et al.* Ferric saccharate induces oxygen radical stress and endothelial dysfunction *in vivo*. *Eur J Clin Invest* 2002;32(Suppl 1):9–16.
- Kuo KL, Hung SC, Lee TS, *et al.* Iron sucrose accelerates early atherogenesis by increasing superoxide production and upregulating adhesion molecules in CKD. *J Am Soc Nephrol* 2014;25:2596–2606.
- Agarwal R, Vasavada N, Sachs NG, *et al.* Oxidative stress and renal injury with intravenous iron in patients with chronic kidney disease. *Kidney Int* 2004;65:2279–2289.
- Agarwal R. Proinflammatory effects of iron sucrose in chronic kidney disease. *Kidney Int* 2006;69:1259–1263.
- Ikeda Y, Ozono I, Tajima S, *et al.* Iron chelation by deferoxamine prevents renal interstitial fibrosis in mice with unilateral ureteral obstruction. *PLoS ONE* 2014;9:e89355.
- Asada N, Takase M, Nakamura J, *et al.* Dysfunction of fibroblasts of extrarenal origin underlies renal fibrosis and renal anemia in mice. *J Clin Invest* 2011;121:3981–3990.
- Souma T, Yamazaki S, Moriguchi T, *et al.* Plasticity of renal erythropoietin-producing cells governs fibrosis. *J Am Soc Nephrol* 2013;24:1599–1616.
- Obara N, Suzuki N, Kim K, *et al.* Repression via the GATA box is essential for tissue-specific erythropoietin gene expression. *Blood* 2008;111:5223–5232.
- Chiang CK, Tanaka T, Inagi R, *et al.* Indoxyl sulfate, a representative uremic toxin, suppresses erythropoietin production in a HIF-dependent manner. *Lab Invest* 2011;91:1564–1571.
- Nagai T, Yasuoka Y, Izumi Y, *et al.* Reevaluation of erythropoietin production by the nephron. *Biochem Biophys Res Commun* 2014;449: 222–228.
- Asai H, Hirata J, Hirano A, *et al.* Activation of aryl hydrocarbon receptor mediates suppression of hypoxia-inducible factor-dependent erythropoietin expression by indoxyl sulfate. *Am J Physiol Cell Physiol* 2016;310:C142–C150.
- Ikeda Y, Enomoto H, Tajima S, *et al.* Dietary iron restriction inhibits progression of diabetic nephropathy in db/db mice. *Am J Physiol Renal Physiol* 2013;304:F1028–F1036.

23. Ikeda Y, Hamano H, Satoh A, *et al*. Bilirubin exerts pro-angiogenic property through Akt-eNOS-dependent pathway. *Hypertens Res* 2015;38:733–740.
24. Hirayama T, Okuda T, Nagasawa H. A highly selective turn-on fluorescent probe for iron(II) to visualize labile iron in living cells. *Chem Sci* 2013;4:1250–1256.
25. Mukaide T, Hattori Y, Misawa N, *et al*. Histological detection of catalytic ferrous iron with the selective turn-on fluorescent probe RhoNox-1 in a Fenton reaction-based rat renal carcinogenesis model. *Free Radic Res* 2014;48:990–995.
26. Rankin EB, Biju MP, Liu Q, *et al*. Hypoxia-inducible factor-2 (HIF-2) regulates hepatic erythropoietin *in vivo*. *J Clin Invest* 2007;117:1068–1077.
27. Paliege A, Rosenberger C, Bondke A, *et al*. Hypoxia-inducible factor-2 α -expressing interstitial fibroblasts are the only renal cells that express erythropoietin under hypoxia-inducible factor stabilization. *Kidney Int* 2010;77:312–318.
28. Kramann R, DiRocco DP, Humphreys BD. Understanding the origin, activation and regulation of matrix-producing myofibroblasts for treatment of fibrotic disease. *J Pathol* 2013;231:273–289.
29. Kruszewski M. Labile iron pool: the main determinant of cellular response to oxidative stress. *Mutat Res* 2003;531:81–92.
30. Appelhoff RJ, Tian YM, Raval RR, *et al*. Differential function of the prolyl hydroxylases PHD1, PHD2, and PHD3 in the regulation of hypoxia-inducible factor. *J Biol Chem* 2004;279:38458–38465.
31. Iwano M, Neilson EG. Mechanisms of tubulointerstitial fibrosis. *Curr Opin Nephrol Hypertens* 2004;13:279–284.
32. Ishizaka N, Saito K, Furuta K, *et al*. Angiotensin II-induced regulation of the expression and localization of iron metabolism-related genes in the rat kidney. *Hypertens Res* 2007;30:195–202.
33. Naito Y, Sawada H, Oboshi M, *et al*. Increased renal iron accumulation in hypertensive nephropathy of salt-loaded hypertensive rats. *PLoS ONE* 2013;8:e75906.
34. Naito Y, Fujii A, Sawada H, *et al*. Association between renal iron accumulation and renal interstitial fibrosis in a rat model of chronic kidney disease. *Hypertens Res* 2015;38:463–470.
35. Semenza GL, Neifelt MK, Chi SM, *et al*. Hypoxia-inducible nuclear factors bind to an enhancer element located 3' to the human erythropoietin gene. *Proc Natl Acad Sci USA* 1991;88:5680–5684.
36. Kapitsinou PP, Liu Q, Unger TL, *et al*. Hepatic HIF-2 regulates erythropoietic responses to hypoxia in renal anemia. *Blood* 2010;116:3039–3048.
37. Warnecke C, Zaborowska Z, Kurreck J, *et al*. Differentiating the functional role of hypoxia-inducible factor (HIF)-1 α and HIF-2 α (EPAS-1) by the use of RNA interference: erythropoietin is a HIF-2 α target gene in Hep3B and Kelly cells. *FASEB J* 2004;18:1462–1464.
38. Semenza GL. HIF-1 and mechanisms of hypoxia sensing. *Curr Opin Cell Biol* 2001;13:167–171.
39. Wang GL, Jiang BH, Semenza GL. Effect of altered redox states on expression and DNA-binding activity of hypoxia-inducible factor 1. *Biochem Biophys Res Commun* 1995;212:550–556.
40. Ho VT, Bunn HF. Effects of transition metals on the expression of the erythropoietin gene: further evidence that the oxygen sensor is a heme protein. *Biochem Biophys Res Commun* 1996;223:175–180.
41. Knowles HJ, Raval RR, Harris AL, *et al*. Effect of ascorbate on the activity of hypoxia-inducible factor in cancer cells. *Cancer Res* 2003;63:1764–1768.
42. Kaelin Jr WG, Ratcliffe PJ. Oxygen sensing by metazoans: the central role of the HIF hydroxylase pathway. *Mol Cell* 2008;30:393–402.
43. Huang LE, Arany Z, Livingston DM, *et al*. Activation of hypoxia-inducible transcription factor depends primarily upon redox-sensitive stabilization of its α subunit. *J Biol Chem* 1996;271:32253–32259.
44. Wiesener MS, Turley H, Allen WE, *et al*. Induction of endothelial PAS domain protein-1 by hypoxia: characterization and comparison with hypoxia-inducible factor-1 α . *Blood* 1998;92:2260–2268.
45. Fandrey J, Frede S, Jelkmann W. Role of hydrogen peroxide in hypoxia-induced erythropoietin production. *Biochem J* 1994;303(Pt 2):507–510.
46. Page EL, Robitaille GA, Pouyssegur J, *et al*. Induction of hypoxia-inducible factor-1 α by transcriptional and translational mechanisms. *J Biol Chem* 2002;277:48403–48409.
47. Wilkinson N, Pantopoulos K. IRP1 regulates erythropoiesis and systemic iron homeostasis by controlling HIF2 α mRNA translation. *Blood* 2013;122:1658–1668.
48. Tovbin D, Mazor D, Vorobiov M, *et al*. Induction of protein oxidation by intravenous iron in hemodialysis patients: role of inflammation. *Am J Kidney Dis* 2002;40:1005–1012.